LAWRENCE
LIVERMORE
NATIONAL
LABORATORY

LLNL-TR-423504

Evaluation of the n + 3H Cross Section at En=14 MeV

P. Navratil, S. Quaglioni, J. D. Anderson, F. S. Dietrich, D. P. McNabb, G. M. Hale

February 11, 2010

Disclaimer

This work performed under the auspices of the U.S. Department of Energy by Lawrence Livermore National Laboratory under Contract DE-AC52-07NA27344.

Evaluation of the n + ^{3}H cross section at E_n=14 MeV

P. Navratil, S. Quaglioni, J. D. Anderson, F. S. Dietrich, D. P. McNabb
Lawrence Livermore National Laboratory

G. M. Hale
Los Alamos National Laboratory

Abstract

The n + ^{3}H cross section is important for NIF diagnostics. As the d-^{3}H fusion at NIF generates neutrons with an energy of 14 MeV, the precise knowledge of the n + ^{3}H cross section and in particular the elastic cross section at that energy is crucial. Experimental data at E_n=14 MeV are not accurate with large disagreements among different sets of measurements. On the other hand, the mirror reaction p-^{3}He is well studied and accurate data are available in a wide range of proton energies. We use several theoretical approaches to evaluate the n-^{3}H cross section by fine-tuning the theory to reproduce the p-^{3}He elastic differential cross sections. The good agreement between the R-matrix analysis and scaled *ab initio* calculations gives us confidence that our evaluated n + ^{3}H cross section is accurate with an uncertainty on the order of 5%.

The fusion of deuterons with tritons in the ^{3}H(d,n)^{4}He reaction at NIF produces neutrons with an energy E_n of 14 MeV. The precise knowledge of the n + ^{3}H cross section and in particular the elastic cross section at E_n=14 MeV is important for NIF diagnostics. Experimental data at this energy are not accurate. This is demonstrated in Fig. 1 that shows data sets from different measurements. Clearly, the data sets are inconsistent, which makes an evaluation of the cross section based purely on data extremely challenging.

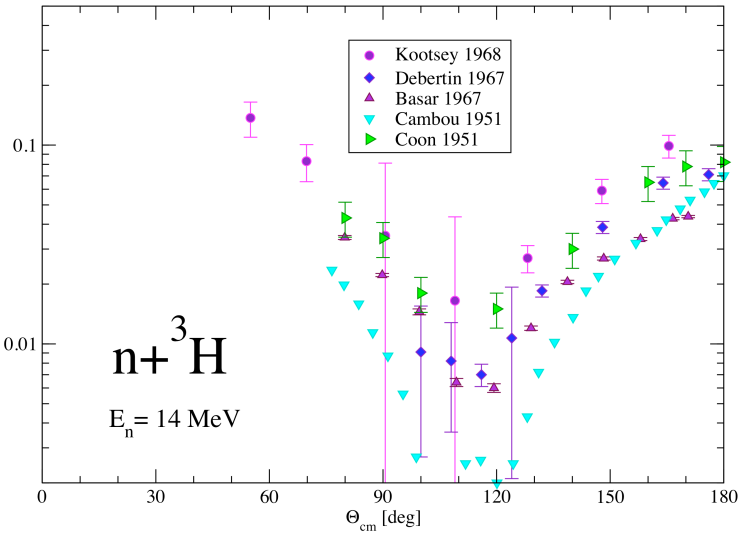

Figure 1. The n+^{3}H elastic differential cross section (in b/sr) at 14 MeV. Available experimental data sets are compared.

A theoretical understanding of n+^{3}H scattering based on first principles calculations is within reach in particular at lower energies, below the ^{3}H breakup threshold. In Fig. 2 (solid red line), we show an example of *ab initio* variational calculation using the hyperspherical harmonics (HH) basis expansion.[1] These calculations, performed with a modern nuclear Hamiltonian consisting of an accurate nucleon-nucleon potential and a three-nucleon interaction, which was developed at LLNL,[2] provide an excellent description of n+^{3}H scattering.

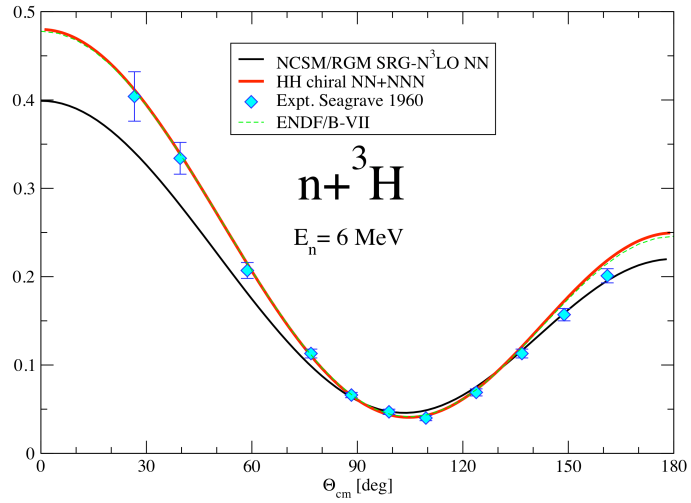

Figure 2. The n+^{3}H elastic differential cross section (in b/sr) at 6 MeV. The HH and NCSM/RGM calculations are compared to the experimental data and the ENDF/B-VII evaluation based on the R-matrix fit to the p-^{3}He data.

Here at the LLNL, we are developing another *ab initio* approach to light-ion reactions, applicable to a wider range of processes. The two-cluster version of this approach that combines the *ab initio* no-core shell model and the resonating group method, called NCSM/RGM, has already proven to be very promising. Unlike earlier *ab initio* approaches, it allows the *ab initio* calculation of various nucleon-nucleus scattering processes for systems with A>4, i.e., both on s- and p-shell targets.[3,4] In Fig. 2, we compare the differential cross section of the n+^{3}H reaction obtained within the NCSM/RGM (solid black line) to that calculated by the variational HH method discussed above. The differences between the two approaches are mostly due to the virtual breakup of the ^{3}H, which is neglected in the two-cluster version of the NCSM/RGM.

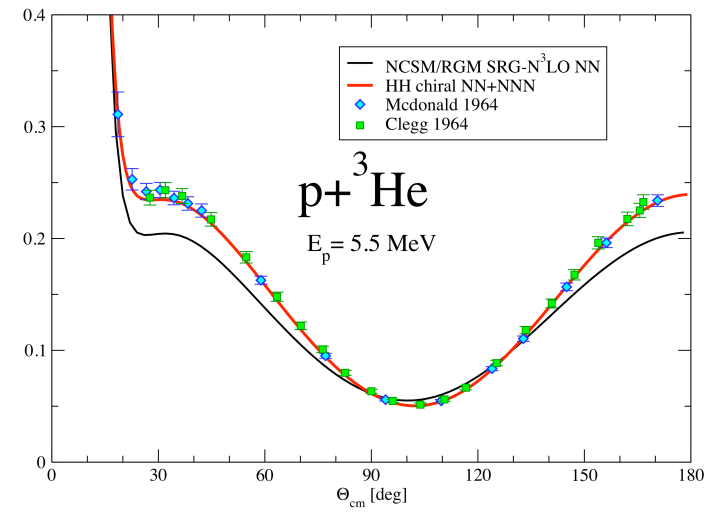

Figure 3. The p+^{3}He elastic differential cross section (in b/sr) at 5.5 MeV. The HH and NCSM/RGM calculations are compared to the experimental data.

We note that there is currently no *ab initio* theory capable of describing the n+^{3}H above the ^{3}H breakup threshold, where one should include the three-cluster final states of the ^{3}H(n,2n)^{2}H reaction. Luckily, in the case of the n+^{3}H reaction, there is a mirror reaction, p+^{3}He, where

accurate experimental data do exist. Examples are shown in Figs. 3 and 4 for energies both below and above the ^{3}He breakup threshold. With the help of existing theories, one can then relate the p+^{3}He and n+^{3}H data and produce a reliable evaluation of the n+^{3}H reaction cross sections even at energies above the ^{3}H breakup.

Fig. 3 demonstrates both the data accuracy and the quality of the p+^{3}He calculations with the same method and Hamiltonian[1,2] as that discussed in Fig. 2. We also show our NCSM/RGM result (solid black line) and observe the same degree of agreement with the HH result (solid red line) as in the n+^{3}H calculations in Fig. 2. While HH calculations are not available at energies above the ^{3}He breakup threshold, we have performed our NCSM/RGM calculations within the present two-cluster approximation also at higher energies. As shown in Fig. 4, we observe a very good description of the data in particular at backward angles.

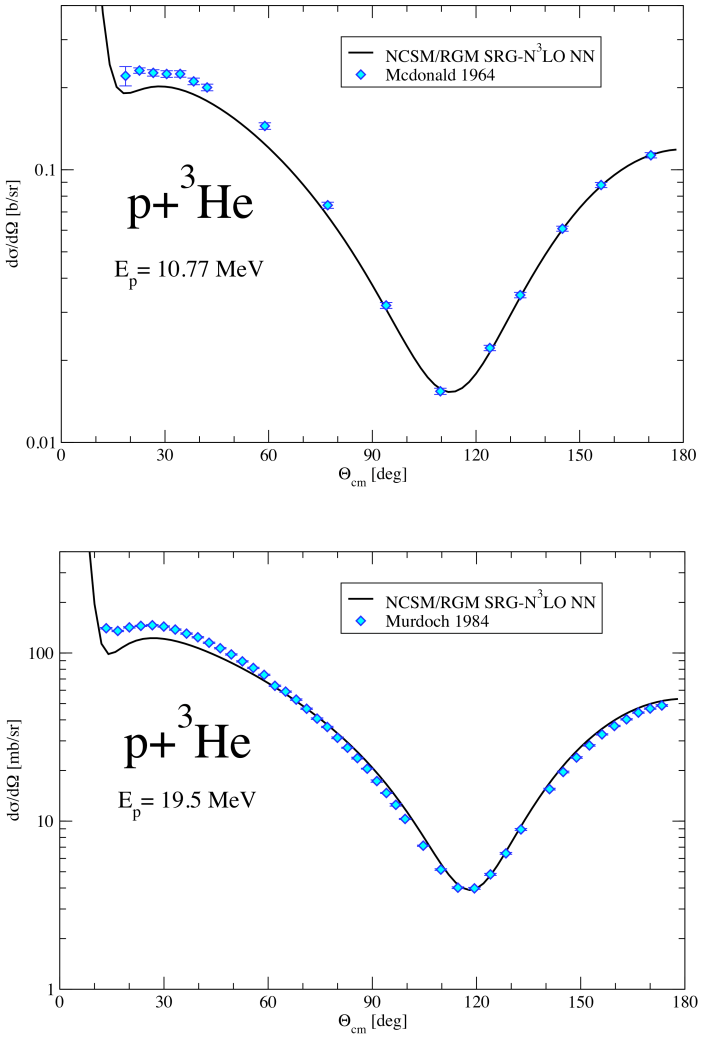

Figure 4. The p+^{3}He elastic differential cross section at 10.77 MeV (upper panel) and 19.5 MeV (lower panel). The NCSM/RGM calculation is compared to the experimental data.

Concerning the n+^{3}H reaction at E_n=14 MeV we are interested in, a very useful experimental data set is that presented in Fig. 5. The p+^{3}He elastic differential cross section was measured with high accuracy at E_p=13.6 MeV.[5] Our NCSM/RGM calculation (solid black line) reproduces the measured cross section very well at angles above 70 degrees. We can now use these data to scale our calculation so that the cross section is also reproduced at angles smaller than 70 degrees. It is sensible to apply the same scaling to our n+^{3}H calculation at E_n=14 MeV as the differences between the two calculations are only in the isospin breaking part of the nucleon-nucleon interaction, which is small compared to the isospin invariant strong part of the nucleon-nucleon potential. To verify that the isospin breaking, i.e. in particular the Coulomb interaction, is treated properly in our calculations, we compare our ratio of the p+^{3}He (Fig. 3) to n+^{3}H (Fig. 2) differential cross sections to the same calculated within the HH variational method. Despite the differences in the approaches and the Hamiltonians, the ratios are in a good agreement as seen in Fig. 6 where the HH ratio is shown by the red dashed line and the NCSM/RGM ratio by the blue dashed-dotted line. This gives us confidence that our p+^{3}He to n+^{3}H ratio at 14 MeV (green solid line in Fig. 6) is accurate. The same scaling inferred from the p+^{3}He data at 13.6 MeV can then be applied to scale the n+^{3}H differential cross section at 14 MeV with confidence. Both the scaled (dashed red line) and the original NCSM/RGM (solid black line) are shown in Fig. 7.

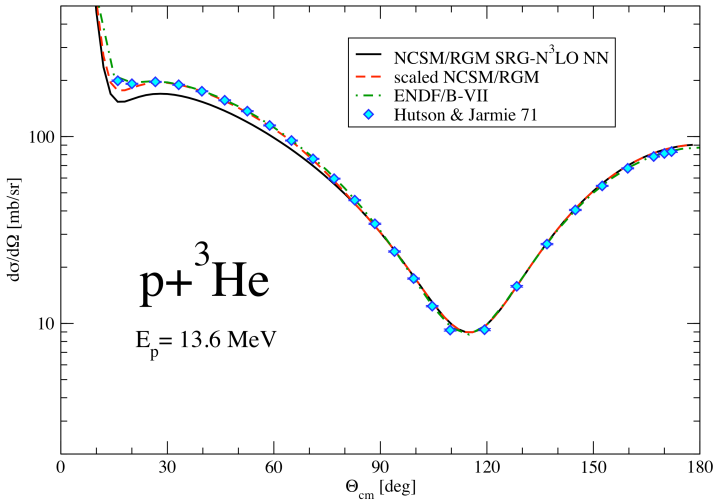

Figure 5. The p+^{3}He elastic differential cross section at 13.6 MeV. The NCSM/RGM calculation (solid black line) is compared to the experimental data of Ref. 5 that are then used to scale the theoretical calculation at forward angles (dashed red line). The ENDF/B-VII evaluation based on the R-matrix fit from Ref. 6 is shown by dashed-dotted green line.

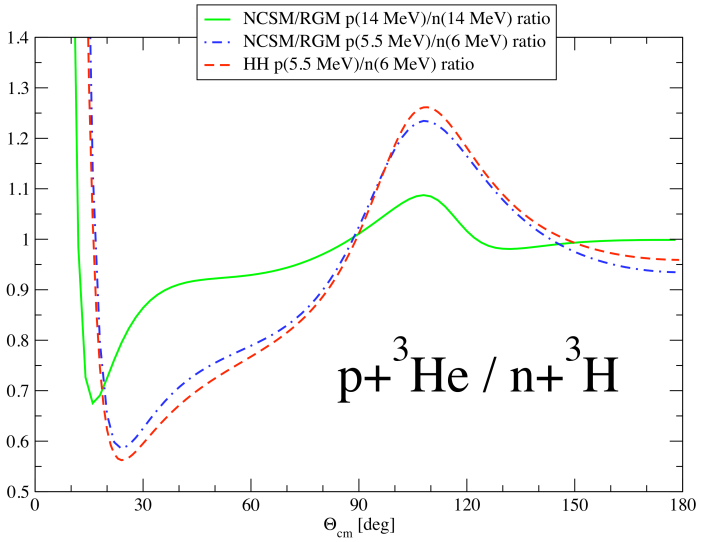

Figure 6. The ratio of p+^{3}He and n+^{3}H elastic cross sections. The NCSM/RGM calculation at 14 MeV (green line) is shown together with a comparison of the NCSM/RGM (blue line) and HH (red line) calculations with 5.5 MeV proton and 6 MeV neutron energies.

Our *ab initio* based results are further compared to the R-matrix analysis of the experimental data that is the basis of the current ENDF/B-VII evaluation. The R-matrix fit was performed for accurate p-^{3}He data in a wide range of energies. The quality of

the fit can be seen in Fig. 5, where the R-matrix analysis differential cross section at 13.6 MeV (green dashed-dotted line) compares extremely well with the experimental points. The R-matrix parameters obtained from the p-^{3}He analysis were then corrected for Coulomb effects as explained in Ref. [6] and applied to the n+^{3}H reaction. The n+^{3}H results agree quite well with the HH calculations at lower energies as demonstrated in Fig. 2 (dotted green line). At the energy of our interest, E_n=14 MeV, the R-matrix analysis elastic cross section prediction (green dashed-dotted line) compares very well with the scaled NCSM/RGM result (red dashed line) as shown in Fig. 7. The largest discrepancy appears at 180 degrees and is on the order of 10%. As seen from the figure, at most other angles the differences are substantially smaller. These differences are due to differing ways of treating Coulomb and other isospin-breaking effects in the two approaches. Taking a conservative view and adopting the average of the two independent results, using their difference rather than the p-^{3}He experimental errors to quantify the

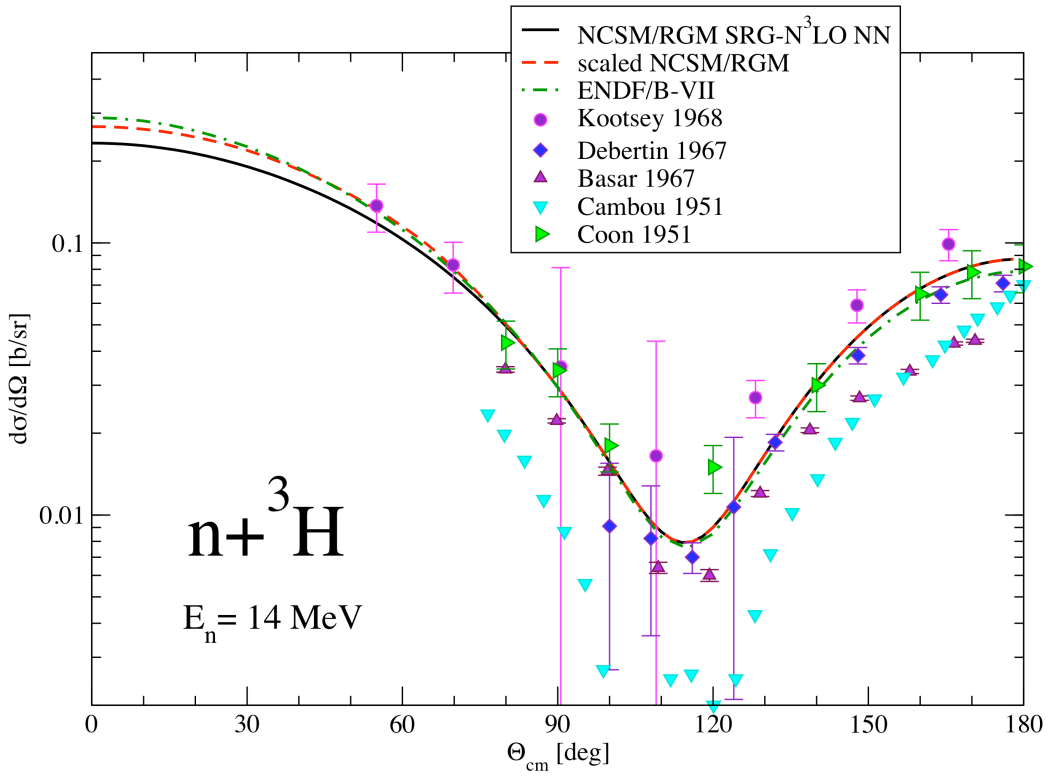

Figure 7. The n+^{3}H elastic differential cross section at 14 MeV. The NCSM/RGM calculation is compared to the experimental data. The dashed line shows the NCSM/RGM calculation scaled by factors obtained from the p+^{3}He results (Fig. 5). The dashed-dotted line represents the ENDF/B-VII evaluation based on the R-matrix analysis of p-^{3}He data.

uncertainty, we arrive at an n+^{3}H cross section that is accurate with an uncertainty on the order of 5%.

The integrated elastic cross section obtained from the scaled NCSM/RGM and the R-matrix is basically identical, equal to 0.94 barn.

Although we believe the combination of R-matrix and NCSM/RGM calculations correctly predicts the 14-MeV n+^{3}H elastic-scattering angular distribution within the stated uncertainties, we need to consider the impact of other (nonelastic) reactions, since they are not included in the NCSM/RGM calculations, and incompletely in the R-matrix. We assume that the magnitude of these processes is very similar for the two reactions, since the 14-MeV projectile energy is far above the threshold for nonelastic processes (8.35 MeV for n+^{3}H; 7.33 MeV for p+^{3}He). This assumption is supported by preliminary calculations[7] of some of the nonelastic channels. Experimental data on nonelastic reactions are unfortunately sparse, and do not contradict our assumption (see e.g. the discussion in Ref. [8]).

We employ a very simple phenomenological complex-potential model (similar to the optical model used in heavier nuclei) to investigate the effects of nonelastic channels, simulated by the imaginary part of the potential in this model. We first fix the parameters of the real part of the potential by fitting the 13.6 MeV p+^{3}He data with no imaginary potential, and then look at the change in the angular distribution when the strength of the imaginary potential is adjusted to yield 45 mb nonelastic cross section. From these results we calculate the ratio of the differential cross section with absorption to that without absorption. The results are shown by the dashed line in Fig. 8 for an average of three different variants of the potential model. Next, we calculate the same quantities for 13.6 MeV n+^{3}H by removing the Coulomb potential but otherwise using exactly the same parameters as determined from p+^{3}He. We find that these calculations also yield 45 mb nonelastic cross section for n+^{3}H, which is in accord with our assumption. The results for n+^{3}H (also an average of the same three potentials used for p+^{3}He) are shown by the solid curve in the figure. Our choice of 45 mb for the nonelastic cross section is taken from the sole measurement of this quantity[9]; however, we believe that additional data would be required to fully settle the issue of the size of this cross section.

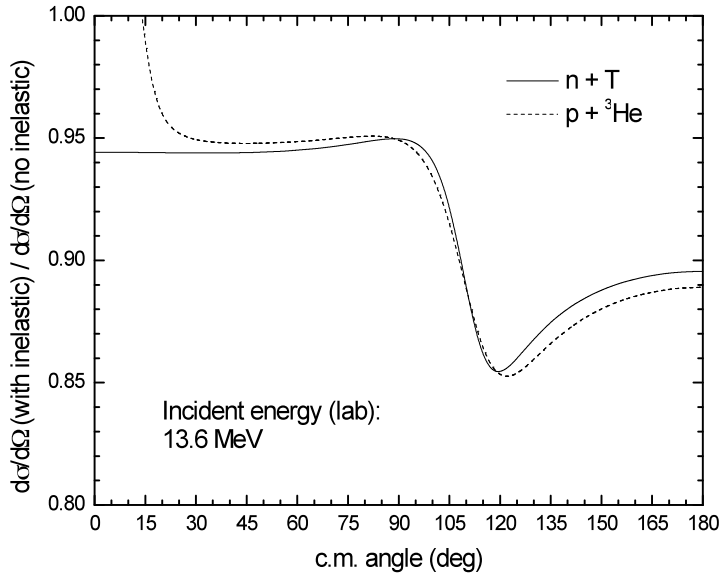

Figure 6. The ratio elastic differential cross sections calculated within the optical model approach with and without the absorption. The p+^{3}He (dotted line) and n+^{3}H (solid line) results at the incident energy of 13.6 MeV are compared. For details see the text.

Aside from small angles (< 20 degrees, which is dominated by Coulomb/nuclear interference effects), the effect of including absorption is very nearly the same (within ~1%) for the two reactions. Therefore, even if more detailed NCSM/RGM calculations including effects of nonelastic channels were to show differences in the angular distributions from the current ones, the agreement of the two curves in the figure suggests that the new calculations could be

normalized to the experimental p+^{3}He data with high confidence that the same normalization should apply to the n+^{3}H calculations. Therefore, we conclude that inclusion of nonelastic effects in future calculations, even if they are as large as those shown in Fig. 8, could be accommodated without significantly changing the present results.

In conclusion, we performed *ab initio* and optical model calculations for the n-^{3}H and p-^{3}He systems. With the help of the accurate p-^{3}He data, we were able to make a prediction of the n-^{3}H elastic differential cross section at E_n=14 MeV. This prediction is in a good agreement with a completely independent R-matrix analysis prediction based on the p-^{3}He data fit. We recommend using the average of the two independently obtained cross sections. Further, we use the two independent predictions to assess the uncertainty of the elastic n-^{3}H cross section, which we find to be less than 5%.

A further improvement of our understanding of the n-^{3}H cross section would require a generalized *ab initio* theory to treat the three-body continuum states in order to describe the ^{3}H breakup. The same generalization is needed to evaluate the ^{3}H(^{3}H,2n)^{4}He cross section with the help of the *ab initio* approach. This is a challenging problem involving large-scale computation.

Acknowledgments
This work was prepared by LLNL under Contract DE-AC52-07NA27344.

Appendix

Table of the recommended elastic n-^{3}He cross section at E_n=14 MeV. The integrated elastic cross section is 0.941 b.

Θ_{CM} [deg]	dσ/dΩ [b/sr]	Prob. distr.	Uncertainty [%]
0	0.2783223	0.2957831	4
5	0.2765281	0.2938764	4
10	0.2713499	0.2883733	4
15	0.2629222	0.2794169	3.5
20	0.2517254	0.2675177	3
25	0.2381245	0.2530635	2.5
30	0.2223896	0.2363415	2.5
35	0.2050979	0.2179649	2.5
40	0.1869702	0.1987	2.5
45	0.1683874	0.1789514	2.5
50	0.1497341	0.1591278	2.5
55	0.1313321	0.1395713	2.5
60	0.1134688	0.1205874	2.5
65	0.096324	0.102367	2.5
70	0.0794901	0.084477	2.5
75	0.0641723	0.0681982	2.5
80	0.0505454	0.0537164	2.5
85	0.0390088	0.041456	2.5
90	0.0294709	0.0313198	2.5
95	0.0216214	0.0229778	2.5
100	0.0154597	0.0164296	2.5
105	0.011098	0.0117943	2.5
110	0.0084981	0.0090312	2.5
115	0.0077487	0.0082348	3
120	0.0087723	0.0093227	3
125	0.011609	0.0123374	3.5
130	0.0161081	0.0171187	4
135	0.0221964	0.0235889	4.5
140	0.0295916	0.0314481	4.5
145	0.0380254	0.040411	5
150	0.0470442	0.0499956	5
155	0.0561495	0.0596721	5
160	0.0647689	0.0688322	5
165	0.0722661	0.0767998	5
170	0.0781317	0.0830334	5
175	0.0818203	0.0869534	5
180	0.0832043	0.0884243	5

[1] M. Viviani, A. Kievski, L. Girlanda, L. E. Marcucci, Few Body Syst. **45**, 119-121 (2009)
[2] P. Navratil, V. G. Gueorguiev, J. P. Vary, W. E. Ormand, A. Nogga, Phys. Rev. Lett. **99**, 042501 (2007); P. Navratil, Few Body Syst. **41**, 117 (2007).
[3] S. Quaglioni and P. Navratil, Phys. Rev. C **79**, 044606 (2009).
[4] S. Quaglioni and P. Navratil, Phys. Rev. Lett. **101**, 092501 (2008).
[5] R. L. Hutson, Nelson Jarmie, J. L. Detch, Jr., and J. H. Jett, Phys. Rev. C **4**, 17 (1971).
[6] G. M. Hale, D. C. Dodder, J. D. Seagrave, B. L. Berman, T. W. Phillips, Phys. Rev. C **42**, 438 (1990).
[7] Ian Thompson, private communication.
[8] A. M. Sourkes, A. Houdayer, W. T. H. van Oers, R. F. Carlson, and. R. E. Brown, Phys. Rev. C 13, 451 (1976).
[9] D. S. Mather and L. F. Pain, AWRE Report No. 047/69, Aldermaston, UK, 1969.